

Fatigue life time modelling of Cu and Au fine wires

Golta Khatibi^{1,*}, *Ali Mazloum-Nejadari*², *Martin Lederer*¹, *Mitra Delshadmanesh*¹ and *Bernhard Czerny*¹

¹Christian Doppler Laboratory for Lifetime and Reliability of Interfaces in Complex Multi-Material Electronics, Institute for Chemical Technologies and Analytics, TU Wien, 1060 Vienna, Austria

²Infineon Technologies AG, Neubiberg, Germany

Abstract. In this study, the influence of microstructure on the cyclic behaviour and lifetime of Cu and Au wires with diameters of 25µm in the low and high cycle fatigue regimes was investigated. Low cycle fatigue (LCF) tests were conducted with a load ratio of 0.1 and a strain rate of $\sim 2e-4$. An ultrasonic resonance fatigue testing system working at 20 kHz was used to obtain lifetime curves under symmetrical loading conditions up to very high cycle regime (VHCF). In order to obtain a total fatigue life model covering the low to high cycle regime of the thin wires by considering the effects of mean stress, a four parameter lifetime model is proposed. The effect of testing frequency on high cycle fatigue data of Cu is discussed based on analysis of strain rate dependency of the tensile properties with the help of the material model proposed by Johnson and Cook.

1 Introduction

Fine metallic Cu and Au wires with diameters in the range of 15 µm to 75 are used for electrical connection between the semiconductor chip and the package in microelectronic devices. The wire bonded interconnects are most commonly made by thermosonic ball bonding technology [1]. During the operation, wire bonds are exposed to repetitive thermal and mechanical cyclic loading as a consequence of thermal extension and contraction of the materials in the package. Gradual accumulation of the plastic strain results in fatigue and final fracture of the wires and failure of the devices. During the thermosonic bonding, electronic flame-off process is applied to melt the tip of the wire by an electrical discharge and to form a free air ball (FAB) which is ultrasonically bonded to the substrate. The FAB process results in formation of a heat affected zone in the wire above the bonded area consisting of recrystallized larger grains. The inhomogeneity of the final microstructure along the wire bond loop depends on the processing condition and the microstructure of the wire prior to the bonding process [1]. The coarse grained heat affected area above the ball bond has been recognized as one of the vulnerable sites of the electronic packages [2]. Knowledge of static and cyclic behaviour of wires in the actual dimensions and microstructure is an important factor for reliable modelling and lifetime prediction of the packages. For automotive and high power electronics with required fault free performance of above 10 years, characterization of the fatigue properties from the low cycle (LCF) up to very high cycle regime (VHCF) is of high importance.

The influence of sample size and microstructure on the static mechanical properties of miniaturized materials has

been extensively studied by using micro tensile-, compression tests or nano-indentation techniques. It was found that the number of grains in the sample volume or the ratio of thickness to grain size plays a major role on the mechanical response of small scaled materials [3]. Due to their high aspect ratio, investigation of the fatigue properties of thin wires requires especial experimental set-ups. Providing the perfect axial alignment and avoiding the buckling of the wire requires special care. Thus fatigue studies on thin wires have been conducted mostly under bending or torsional modes [4,5] and to a very less extent in tension-tension or tension-compression loading modes [6-9]. Studies on the high cycle fatigue behaviour of thin micro wires are very scarce [9].

In the last decades, ultrasonic fatigue testing has been used as an established time saving method for investigation of VHCF behaviour of a wide range of materials. The effect of high strain rate / high frequency loading on the static and dynamic response of materials has been subject of experimental and theoretical studies [10,11]. The influence of strain rate and testing frequency on the tensile and fatigue properties of copper as a reference material has been studied more extensively with the results being partly controversial [10-15].

In the present study the influence of microstructure and mechanical properties of thin Au and Cu wires on their low and high cycle fatigue response was studied. The LCF stress controlled experiments were conducted at low strain rates (<1Hz). Using an ultrasonic resonance testing system working at 20 kHz allowed to perform fully reversed HCF experiments up to $1e9$ loading cycles. Based on the experimental data and analytical approach, the effects of mean stress and the strain rate on the lifetime of Au and Cu micro wires is discussed. A lifetime model

* Corresponding author: golta.khatibi@tuwien.ac.at

for Au and Cu fine wires covering the low to high cycle regime is suggested.

2 Materials and Methods

Commercial high purity Cu and Au wires with diameters of 25 μ m which are used for interconnection in microelectronics devices were purchased from different suppliers. The microstructure of the wires was modified by annealing at 450 $^{\circ}$ C for one hour in vacuum. The annealing conditions were selected based on a previous study with the aim to obtain a microstructure similar to that occurring in the heat affected zone of thermosonic wire bonds in microelectronic packages [2]. The wires are denoted as Cu-*i* and Au-*i* for the initial state and Cu-*a* and Au-*a* for the annealed condition.

2.1 Microstructural characterization

The microstructures of the Au and Cu wires in the initial condition (as purchased) are shown in figures 1a-b. The Au and Cu wires exhibited considerably distinct microstructures which were dependent on the processing parameters during the wire drawing. The microstructure and texture of fine Au and Cu wires used in electronic packages in dependency of processing parameters has been subject of a number of extensive investigations [16,17]. In our study, the Au-*i* wires show an inhomogeneous fine grained structure with a recrystallized region at the periphery and a strong fibre textured region in the core. The microstructure of Cu-*i* wires consists of smaller and larger recrystallized equiaxed grains with an average grain size of \sim 10 μ m. Annealing resulted in different degrees of recrystallization and grain coarsening in each material. A quasi-bamboo structured microstructure was obtained for Cu-*a* wires. The microstructure of the annealed Au-*a* samples remained multi-crystalline consisting of a few grains in the cross section of the wires.

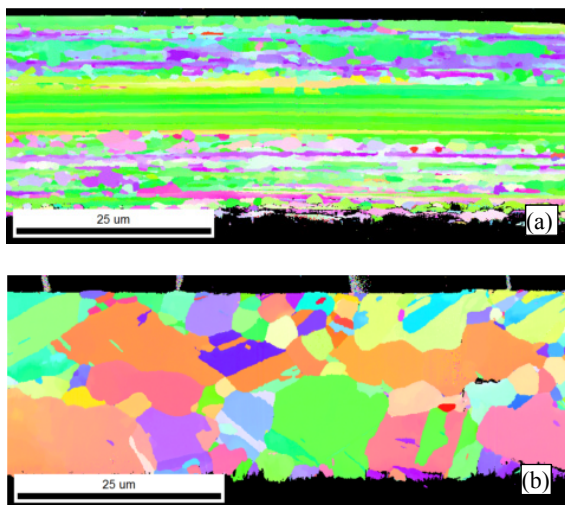


Fig. 1. Microstructure of the (a) Au and (b) Cu micro-wires in the initial state. (EBSD images of the longitudinal sections).

2.2 Tensile and fatigue tests

2.2.1 Tensile test and low cycle fatigue set-up

Tensile properties and Young's Modulus of the Cu wires were determined by using a micro-tensile machine equipped with a load cell with a capacity of 1N and accuracy of \pm 0.001N. A laser speckle extensometer with a strain resolution of about $10e-5$ was used for contactless strain measurements. All tests were conducted at strain rate of $1.3e-4$ s $^{-1}$.

Low cycle fatigue tests were conducted by using the same micro-tensile machine. Load controlled tensile-tensile low cycle fatigue tests were conducted up to about $2e4$ cycles. The stress ratio ($R = \sigma_{min} / \sigma_{max}$) was \sim 0.11 - 0.12 to avoid possible buckling of the wires during the unloading cycles. The tests were started with a strain rate of $1.3e-4$ s $^{-1}$ which was increased to $\sim 2e-4$ s $^{-1}$ after reaching the maximum stress. This testing speed is equivalent to a testing frequency of about 0.05 Hz. LCF curves were obtained from 20- 30 experiments for each sample series. Figure 2 shows the overlapping of the static and cyclic stress-displacement curves for the Cu-*i* fine grained wires. The observed ratcheting was a typical behaviour for the thin wires during the cyclic tension-tension loading (Fig. 2). All the tested wires showed a variation between the monotonic and cyclic fracture strain which was higher for annealed wires with a larger standard deviation of their tensile properties (Table 1) and the cyclic hardening effect.

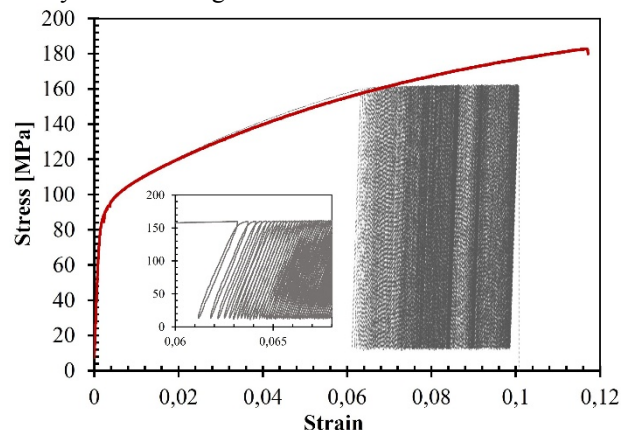


Fig. 2. Cyclic and monotonic stress-displacement curves of Cu-*i* wires with the insert showing the details of the typical ratcheting behaviour of thin wires subjected to tensile-tensile cyclic loading.

2.2.2 High cycle fatigue set-up

High cycle fatigue experiments were performed by using a standard ultrasonic resonance testing system working at 20 kHz which was adapted for testing of miniaturized samples [9]. The resonance system consists of a power supply, a piezoelectric transducer and a mechanical part which includes an acoustic horn. Further, the horn is connected to a sample holder with a resonance length ($\lambda/2$) of 128mm and a cross-section of 20x8 mm 2 . During the loading, the mechanical part of the system is excited to longitudinal push-pull vibrations with a zero mean

strain (i.e. $R = -1$). The distribution of displacement and strain varies in a sinusoidal manner along the system with the maximum of the strain being in the midsection of the holder. The cyclic strain amplitude is determined by using a strain gauge. Two grooves with a width and depth of about $0.3 \times 0.3 \mu\text{m}$ are machined into the both sides of the holder at this location. Fatigue tests are performed by placing and aligning the wires over the groove parallel to the loading direction and gluing them by using a cyanide-acrylate adhesive. Thus the gauge section of the wires across the groove is free-standing. The effective strain amplitude of the wires during the testing was estimated by means of finite element analysis and validated by using a miniaturized strain gauge which was applied over the groove resulting in a stress concentration value (k_t) of 1.3. Under the assumption of preliminarily elastic deformation in the high cycle regime, the cyclic stress amplitude can be obtained from the strain value measured with the strain gauge and the Young's modulus of the wires in accordance with Hooke's law. The loading cycles to failure (N_f) were determined by monitoring the surface of the wires with a high resolution video microscope during the entire testing. The tests were performed at room temperature with additional cooling of the specimen by pressurized dry air.

3 Results

3.1 Tensile properties

The stress-strain curves of the Au and Cu wires prior and subsequent to annealing are presented in figure 3 and the obtained mechanical properties are listed in Table 1. The curves show that the fine grained Au-*i* wires which exhibit the highest yield and tensile strength are highly prone to softening subsequent to annealing at 450°C . The ductility remains low with a value of about 4% for the initial and annealed wires. According to a study on similar wires [17] the high tensile strength of the cold drawn fine Au wires is related to the high percentage of $\langle 111 \rangle$ fibre component in the microstructure. By annealing at the temperature range of 400°C to 700°C the $\langle 100 \rangle$ recrystallization textures is predominantly formed resulting in softening and a decrease of the yield and ultimate tensile strength of the wire. Though annealing also results in a strong decrease of yield and tensile strength of the Cu wires, the wires show the same hardening behaviour.

Table 1. Mechanical properties of Cu and Au micro wires.

Wire material	Yield stress σ_y [MPa]	Tensile strength σ_u [MPa]	Fracture strain [%]	Young's Modulus E [GPa]
Cu - <i>i</i>	63 ± 4.5	178 ± 5	10.4 ± 2	95 ± 4
Cu - <i>a</i>	26 ± 5.3	112 ± 14	4.5 ± 2	78 ± 3
Au - <i>i</i>	130	209 ± 2	3.5 ± 1	75 ± 2
Au - <i>a</i>	31 ± 3	84 ± 5	4.5 ± 2	76 ± 5

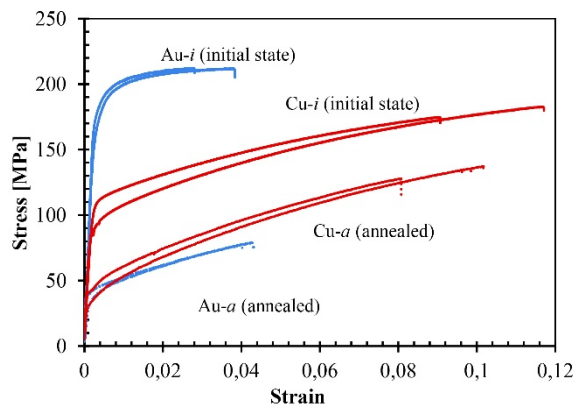


Fig. 3. Stress-strain behaviour of Cu and Au wires prior and after annealing.

3.1.1. Modelling of strain rate dependency

The strain rate dependency of the stress-strain response of the Cu wires was analysed by using the Johnson and Cook constitutive model [10]. The simulations were conducted by using

$$\sigma = (A + B \cdot \epsilon_{pl}^n) \cdot (1 + C \cdot \ln \dot{\epsilon}^*), \quad (1)$$

where A, B, C, and n are material parameters, ϵ_{pl} is the equivalent plastic strain, $\dot{\epsilon}^* = \frac{\dot{\epsilon}}{\dot{\epsilon}_0}$ is the dimensionless

strain rate and $\dot{\epsilon}_0$ is the reference strain rate. The temperature dependent term of the model could be neglected since all the experiments were performed at room temperature. The strain rate dependency of tensile response of Cu wires prior and after annealing for strain rates of $1e-4 \text{ s}^{-1}$ ($\sim 0.05 \text{ Hz}$) and 32 s^{-1} ($\sim 20 \text{ kHz}$) is presented in figure 4 and the model parameters used for the numerical fits are given in table 2. The results show that at lower strain values the yield stress of Cu increases by a factor of $(1 + C \cdot \ln \dot{\epsilon}^*) = 1.32$.

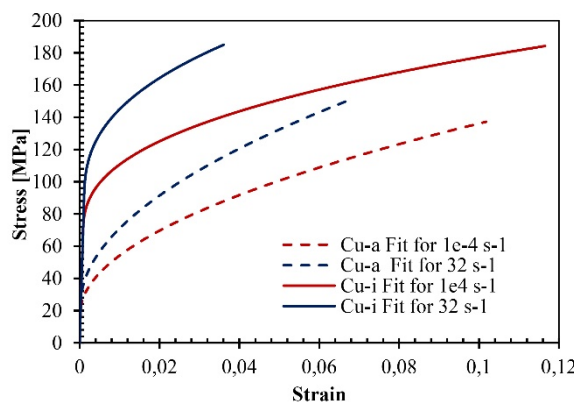


Fig. 4. Johnson and Cook model fits showing the strain rate dependency of Cu wires prior and after annealing.

Table 2. Material parameters for initial and annealed Cu micro wires. The value for C was adopted according to reference [10].

	A [MPa]	B [MPa]	C	n	$\dot{\epsilon}_0$ [s ⁻¹]
Cu -i	70	272	0.025	0.4	1e-4
Cu -a	20	388	0.025	0.52	1e-4

3.1 Fatigue life curves

The influence of microstructure and tensile properties on the low and high cycle fatigue life of Au and Cu micro-wires is presented in figures 5 and 6, respectively. The LCF curves are presented as a function of the stress amplitude against (N_f) up to 2e4 loading cycles (Fig. 5). The results of the fatigue experiments show a direct relationship between their cyclic and monotonic properties for all samples (Fig. 1, Table 1). The best fatigue performance was obtained for the fine grained Au-i wires with a tensile strength (σ_u) of 209 MPa while the lowest lifetime was observed for the annealed Au wires ($\sigma_u = 84$ MPa). For comparison reasons the experimental fatigue data were fitted by using a Basquin type equation,

$$\sigma_a = \sigma'_f (N_f)^{-b} \quad (2)$$

as presented in figure 5. Using equation (2) the stress amplitude σ_a is expressed by a first order power law of loading cycles (N_f) with σ'_f being the fatigue stress coefficient and b being the fatigue stress exponent. The values of σ'_f are determined to be 112 MPa and 35 MPa for initial and annealed Au wires and 93 MPa and 53 MPa for initial and annealed Cu wires, respectively. These coefficients correlate very well to the corresponding $\frac{\sigma_u}{2}$ values for each wire. The stress exponent values which indicate the slopes of the curves are found to be in the range of 0.01 to 0.04. The higher slope may indicate a stronger decrease of fatigue life at intermediate or higher loading cycles.

Previous studies on low cycle fatigue of thin Cu wires [6-7] and lines [8] with diameters /thicknesses in the range of 20 μ m to 95 μ m subjected to alternate tensile loading ($R \sim 0$) reported a similar behaviour. The cyclic properties were found to be closely related to the monotonic tensile response and obey the Basquin law. The fatigue stress exponent (n) was found to be in the range of 0.01-0.07 and the fatigue strength coefficient correlated very well with the tensile strength of the material.

The high cycle fatigue life curves of the four wire materials with $R = -1$ and $f = 20$ kHz are presented in figure 6. The trend of the S-N curves in the range of 5e5 to 1e9 cycles is similar to that found in LCF regime. The highest fatigue resistance is again obtained for Au-i wires with the highest yield and tensile strength. The lifetime curve lies between the stress amplitudes of 53 MPa ($N_f = 1e6$) and 46 MPa which is considered as the fatigue limit at 1e9 cycles. The lifetime curve of Cu-i wires which lies

beneath that of Au-i exhibits a steeper slope with a fatigue limit of 25 MPa at 1e9. Annealing results in a strong reduction of the fatigue resistance of the wires which with a drop of about 50% is more severe for Au-i wires. The lifetime curve of Cu-a wires is slightly higher than that of Au-a wires and the fatigue limit of the both wire series is 15 -16 MPa at 1e9 cycles. In a previous study high cycle fatigue of bamboo structured thin wires of 10 μ m to 125 μ m was investigated by using the same experimental set-up ($R = -1$, frequency 20 kHz) [9]. The authors found that the higher monotonic yield stress results in an improved fatigue resistance in the high cycle regime. This result complies well with the findings of the present work.

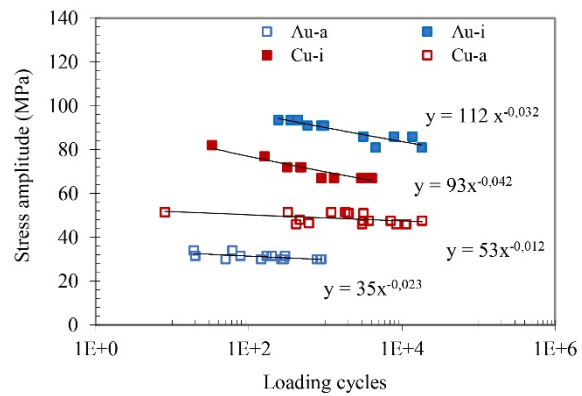


Fig. 5. Comparison of low cycle fatigue life curves of Au and Cu fine wires with different grain sizes in initial and annealed states.

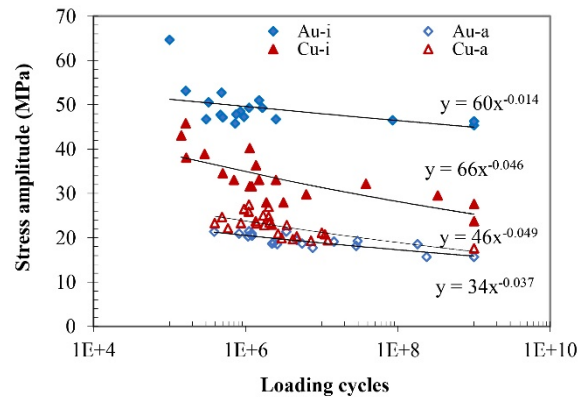


Fig. 6. Comparison of high cycle fatigue life curves of Au and Cu fine wires with different grain sizes in initial and annealed states.

3.1.1 Fracture surface observations

Figures 7 and 8 show the surface morphologies of the Cu wires next to the failure site indicating the effect of microstructure /grain size and the mean stress on the failure modes of the wires. The plastic deformation observed on the surface of the initial and annealed Cu wires subjected to tensile alternating loads resemble strongly to that caused by uniaxial tensile loading (Fig. 7a and 8a respectively). Failure occurs as a result of slip band formation, necking and rupture of the wires in a ductile manner. In the case of Cu-a quasi-bamboo structured wires, plastic deformation has caused formation of slip steps at the grain boundaries of the two grains which have

been individually deformed until final rupture in a knife edge manner. The surface of Cu-*i* (7b) and Cu-*a* (8b) wires exhibit the typical deformation features which are observed on the surface of copper samples subjected to symmetrical cyclic loading. Strong surface roughening due to local slip band formation and deeper intergranular cracks near the ruptured area can be observed on the surface of a Cu-*i* wire (Fig. 7b). Figure 8b indicates that the slip bands have been developed mainly in the large grains with a preferred orientation with respect to the loading axis. Several elliptical shaped slip bands which formed in two large grains indicate a partly bamboo like structure in this region. Similar features were observed on the fatigue fracture surfaces of the Au wires.

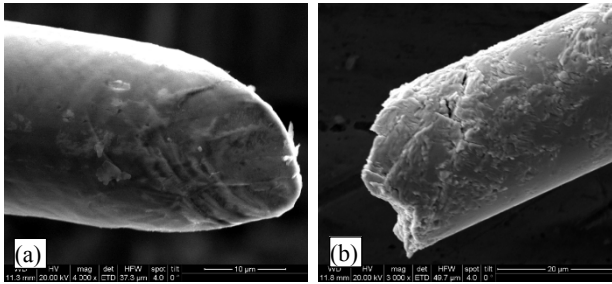


Fig. 7. Typical images of fatigue fracture surfaces of Cu-*i* wires after failure at low and high cycle regime

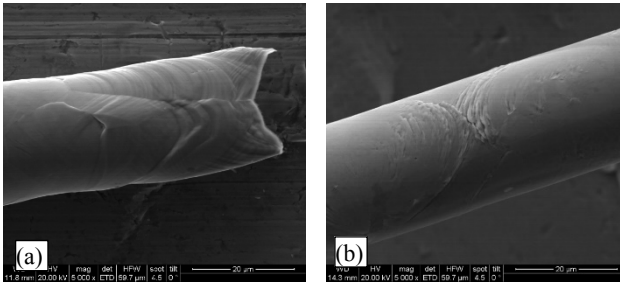


Fig. 8. Typical images of fatigue fracture surfaces of Cu-*a* wires after failure at low and high cycle regime

3.2 Fatigue life modelling

Establishment of lifetime curves covering the low to high cycle regime was conducted based on the experimental results and considering the effect of mean stress [18, 19]. For this purpose Gerber and Goodman methods were used for conversion of the maximum stress σ_{max} at low cycle fatigue tests to an effective stress amplitude σ_e' for symmetrical loading by the following equations:

$$\frac{\sigma_a}{\sigma_e'} + \frac{\sigma_m}{\sigma_u} = 1 \quad (3)$$

$$\frac{\sigma_a}{\sigma_e'} + \left(\frac{\sigma_m}{\sigma_u} \right)^2 = 1, \quad (4)$$

where σ_a , σ_m , and σ_u are the stress amplitude, the mean stress and the ultimate tensile stress in Goodman (3) and Gerber (4) equations, respectively. The results of

transformation of the maximum stress amplitude to an equivalent symmetrical stress amplitude for the low cycle fatigue data for the annealed Au wires is shown in figure 9. The experimental stress amplitude values for low and high cycle fatigue are also included in this plot. It can be observed that the Gerber model provides a more conservative result.

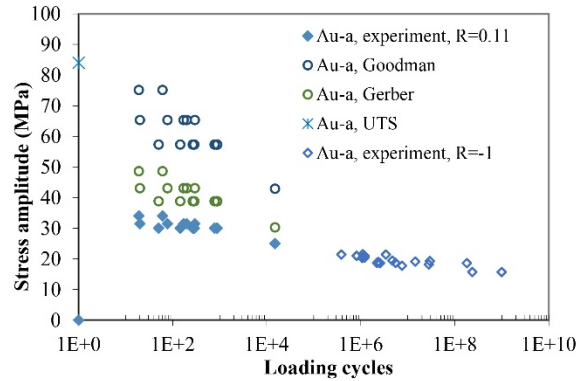


Fig. 9. Conversion of σ_{max} from LCF experiments to symmetrical stress amplitude values $\Delta\sigma/2$ ($R=-1$) based on using the Goodman and Gerber equations for Au-*i* wires.

The total fatigue life curves for Au and Cu wires for symmetrical loading conditions ($R=-1$) are presented in figures 10 and 11 based on the converted LCF data by using the Goodman equation and the obtained experimental HCF values. According to the Johnson and Cook material models proposed for the initial and annealed Cu wires (Table 2, Fig. 4), loading at a testing frequency of 20 kHz ($\sim 32 \text{ s}^{-1}$) results in an increase of the yield stress level of Cu by a factor of 1.32 at relative low strains. However this effect occurs after yielding of the material. In this study, the maximum stress amplitudes of the high cycle fatigue data in the whole loading range were found to be below the yield strength of all the wires. Thus an increase or shift of the experimentally determined lifetime curves due to testing at 20 kHz is not expected or it can be considered as negligible. Though the strain rate dependency of stress-strain response of Au wires have not been calculated in this work, concerning the HCF curves, similar arguments may also be applied. Detailed investigation of the influence of cyclic testing frequency on fatigue response of copper can be found in [13-15, 20]. In order to establish lifetime models covering the low and high cycle fatigue range of the Au and Cu micro wires, a four parameter lifetime model originally proposed by Weibull was used. The lifetime model is based on the equation (5):

$$S(N) = S_d + \frac{S_{max} - S_d}{\exp\left\{\left(\frac{\log(N)}{\alpha}\right)^\beta\right\}}, \quad (5)$$

where $S(N)$ is the stress amplitude, S_{max} is the ultimate tensile strength, S_d is the endurance limit of the material, N is the number of loading cycles to failure, α and β are material parameters. The parameters used for the model are given in Table 3 and the obtained lifetime models for Cu and Au wires prior and subsequent to annealing are presented in figures 10 and 11, respectively. The lifetime

models for Au-*i* and Cu-*i* wires show a steep slope in the low and intermediate region resulting in a rather abrupt drop of fatigue resistance at higher loading cycles. The annealed Cu-*a* wires show a moderate decrease of fatigue resistance in the transition region from LCF to HCF regime. The fatigue curve of the Au-*a* wires with the weakest mechanical properties follows a flat trend in the whole range of lifetime.

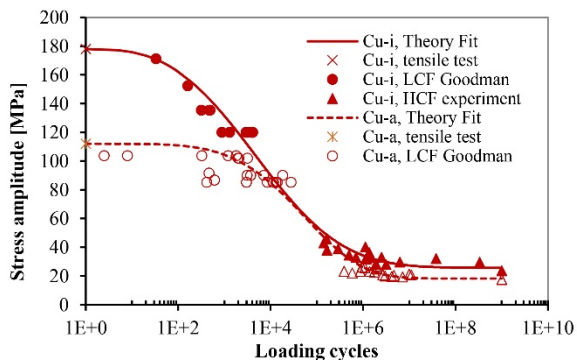


Fig. 10. Lifetime model for Cu fine wires prior and after annealing

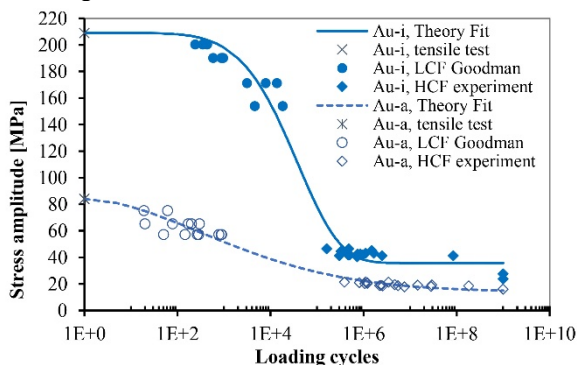


Fig. 11. Lifetime model for Au fine wires prior and after annealing

Table 3. Material parameters for lifetime models of the initial and annealed Cu and Au wires.

Wire material	S_d [MPa]	α	β
Cu- <i>i</i>	25.69	9.6916	2.9736
Cu- <i>a</i>	18.2	11.4741	4.8556
Au- <i>i</i>	35.71	10.8762	5.9965
Au- <i>a</i>	14.22	8.9872	1.789

The lifetime curves of the Au and Cu wires in the initial state are representative for the fatigue response of a typical wire bond in the region along the loop further from the bonded area, while the lifetime curves of the annealed wires estimate the fatigue performance of the heat affected zone above the ball bond [1,2].

4 Summary and Conclusion

In this study the influence of grain size, strain rate and loading mode on the tensile and fatigue properties of gold

and copper micro wires used as interconnects in microelectronic packages have been investigated. Based on the experimental stress-strain curves and using the Johnson and Cook model, the strain rate dependency of material properties of Cu wires were assessed at strain rates of $1e-4 \text{ s}^{-1}$ and 32 s^{-1} . LCF and HCF experiments were performed with $R=0.1$ at $\sim 0.05 \text{ Hz}$ ($1e-4 \text{ s}^{-1}$) and $R=-1$ at 20 kHz ($\sim 32 \text{ s}^{-1}$), respectively. The effect of mean stress was considered based on the Goodman equation which was used for conversion of the maximum stress of the LCF tests to an effective stress amplitude for symmetrical loading. The maximum stress (stress amplitude) during the HCF loading at 20 kHz remained below the yield strength of the material. Thus, based on the calculated strain rate material model for copper, the effect of high strain rate on the response to cyclic loading of the samples was considered to be negligible. Further experiments on the effect of testing frequency on the fatigue life of Cu and Au micro wires are going on. Finally, by using the experimental low and high cycle fatigue curves, total lifetime models for Au and Cu wires of $25 \mu\text{m}$ could be established. Depending on the expected service conditions, the proposed lifetime models may serve as a tool for a proper material choice for thermosonic ball bonds in electronic packages.

Acknowledgements: The financial support by the Austrian Federal Ministry for Digital and Economic Affairs and the National Foundation for Research, Technology and Development is gratefully acknowledged. The authors would like to thank A. Steiger Thirsfeld from USTEM-TU Wien for the EBSD images.

References

1. Copper Wire Bonding, P. S. Chauhan, A. Choubey, Z. W. Zhong, M. G. Pecht, Springer (2013)
2. A. Mazloun-Nejadari, G. Khatibi, B. Czerny, M. Lederer, J. Nicolics, L. Weiss, Microelectron. Reliab., 74 (2017) 147-154
3. B. Weiss, V. Gröger, G. Khatibi, A. Kotas, P. Zimprich, R. Stickler, B. Zagar, Sens. Actuators, A 3287, (2002) 1-11
4. A. Schreiner, J.T. Mortimer, T.P. Kicher, J Biomed Mater Res. 25 (1991) 589-608
5. Z. H. Zhao, C.Q. Feng, S. Zhao, M. Lei, Key Eng. Mater. 734 (2017) 176-184
6. R. Hofbeck, K. Hausmann, B. Ilshner, H.U. Künzi, Scripta Metallurgica (1986) 20 : 1601-1605
7. B. Yang, C. Motz, W. Grosinger, G. Dehm, Mater. Sci. Eng. A 515 (2009) 71-78
8. A. Wimmer, A. Leitner, T. Detzel, W. Robl, W. Heinz, R. Pippan, G. Dehm, Acta Mater. 67 (2014) 297-307
9. G. Khatibi, A. Betzwar-Kotas, V. Göger, B. Weiss, Fatigue Fract. Eng. Mater. Struct. 28 (2005) 723-73
10. G. R. Johnson, W. H. Cook, Proc. 7th Int Symp on Ballistics (1983)541-47
11. C. Laird, P. Charsley, in J.M Wells, O. Buck, L.D. Roth, J.K. Tien (Eds.), Ultrasonic Fatigue, The

- Metall. Soc. of AIME, Philadelphia (1982), pp. 187-205
12. J.S. Kim and H. Huh, *Experimental Mechanics* (2011) 51:845–855
 13. S. Stanzl-Tschegg, *Int. J. Fatigue*, 105(2017) 86-96
 14. P. Lukáš, L. Kunz, Z. Knésl, B. Weiss, R. Stickler, *Mater. Sci. Eng.* 70 (1985) 91-100
 15. L. Kunz, in *Copper alloys - Early applications and current performance - Enhancing processes*, in: L. Collini (Ed.), InTech, Rijeka, Croatia, (2012) 93–126
 16. J.H. Cho, A.D. Rollet, J.S. Cho, Y.J. Park, J.T. Moon, K.H. Oh, *Metall. Mater. Trans. A*, 37A (2006) 3085-3097
 17. S.H. Kang, H.S. Jung, W.H. Bang, J.H. Cho, K.H. Oh *et al.*, *Mater. Sci. Forum* 1 (2005) 495-497
 18. R. Eckert, C. Laird, J. Bassani, *Mater. Sci. Eng.* 91 (1987) 81-88
 19. H. Hwangbo, J.H. Song, *Mater. Sci. Eng. A* 527 (2010) 2222-2232
 20. H. Mayer, C. Laird, *Mater. Sci. Eng.* A187 (1994) 23-35